Design of Multiple Beam Forming Antenna System Using Substrate Integrated Folded Waveguide (SIFW) Technology

Wriddhi Bhowmik[1, *], Shweta Srivastava[1], and Laxman Prasad[2]

Abstract—This paper introduces a novel structure of 4×4 multiple beam forming antenna system using substrate integrated folded waveguide technology. For high speed wireless communication it is necessary to minimize the interferences and multipath fading. Multiple beam forming antenna system is a good solution to these problems. The substrate integrated folded waveguide (SIFW) technology reduces the width of substrate integrated waveguide (SIW) by half. All the basic building blocks required for the antenna array system are designed and simulated individually. They are then combined to form the butler matrix fed antenna array system. The SIFW technology reduces the total width of butler matrix. The radiation performance of the multiple beam forming antenna system is realized by integrating the H-plane SIFW horn antennas with the output ports of the butler matrix. The system is practically realized and good directive multiple beams with symmetric gain (5.8 dB, 5.63 dB, 5.31 dB and 5.9 dB for the beams 1R, 2L, 2R and 1L) have been achieved.

1. INTRODUCTION

A high speed wireless communication system requires minimum interference and multipath fading as well as improved channel capacity. Frequency reuse technique is a suitable option to enhance the channel capacity of a system and that can be attained by multiple directive beams. Multiple beam forming antenna systems (M-BFAS) are the key solutions to meet these essential requirements. These systems are used frequently in space division multiple access (SDMA) applications [1]. The M-BFAS are equipped with the multiple beam forming network (M-BFN) and the antenna elements. Several beam formers are available in literature such as Blass matrix, Nolen matrix and Rotman lens and Butler matrix [2–4]. The efficiency of Blass matrix and Rotman lens are quite low due to high losses associated with the structures. Among these, the Butler matrix array is most popular due to low loss as well as very few components required for the system implementation [5].

Earlier microstrip technique was used to implement the Butler matrix array to make the system compact, light weight and less expensive. 3 dB branch line coupler, crossover or 0 dB coupler and 45° phase shifter are considered as the key components to realize the Butler matrix array. Generally the rectangular patch microstrip antennas have been used as the radiating elements, fed by the output ports of Butler matrix array to trigger the directive beams [6–10]. But at high frequencies the ohmic and dielectric losses are quite large in the microstrip feeding network. Also the undesired radiation of feeding network degrades the radiation performance of M-BFAS. At high frequencies waveguide technology is used to develop the Butler matrix array [11]. But the non planar structure of rectangular waveguide makes the system bulky, expensive and difficult to integrate with other components.

The substrate Integrated Waveguide (SIW) technology is an alternate way to implement the rectangular waveguide in planar form. This technology preserves all the advantages of rectangular waveguide and also make the system compact, light weight and less expensive. Recently some researchers

---

* Corresponding author: Wriddhi Bhowmik (bhowmikwriddhi@gmail.com).
[1] Department of Electronics and Communication Engineering, Birla Institute of Technology, Mesra, Ranchi, India. [2] Department of Electronics and Communication Engineering, Raj Kumar Goel Institute of Technology, Ghaziabad, U.P., India.

have realized the Butler matrix array on PCB using SIW technology [12–15]. In [12, 13] a single layer implementation has been reported. Other researchers [14, 15] have eliminated the use of 0 dB coupler by using multilayered design. The multilayered structure reduces the size of the Butler matrix. Layer to layer transitions have been used to connect the SIW's in different layers which makes the system more complex. Slight displacement of the layers might affect the measurements.

To reduce the design complexity without affecting the performance of beam forming antenna system, a Butler matrix array can be designed using substrate integrated folded waveguide technique. In the proposed work a substrate integrated folded waveguide multiple beam forming antenna system is presented. The substrate integrated folded waveguide (SIFW) technology reduces the width of the SIW to half for the same cut-off frequency. The H-plane SIFW double slot 3 dB and 0 dB coupler and the H-plane SIFW 45° phase shifter are designed as the basic building blocks of the Butler matrix array. The proposed structure is designed on a polytetrafluoroethylene (PTFE) substrate with a dielectric constant (ε_r) of 2.5, thickness (h) of 0.5 mm and loss tangent ($\tan \delta$) of 0.00015. The simulations have been carried out by using commercial HFSS software. The H-plane SIFW horn antenna has been designed as the radiating element. Using the horn as the radiating element eliminates the transitions required for feeding the patch antennas. The output ports of the proposed Butler matrix network feed the antenna elements and the specific phase differences between the output ports of BFN make the M-BFAS capable to generate the directive beams in the different end fire directions. The SIFW technology does not use multiple layers, hence it eliminates the utilization of layer to layer transitions as well as the losses responsible for these transitions, also reducing the fabrication difficulties.

Earlier papers reported the radiation performance of the antenna array system analytically; simulations and measurements have not been carried out to validate the analysis. The proposed work combines the H-plane SIFW horn antenna with SIFW Butler matrix array to achieve the multiple directive beams practically. The radiation performance of the proposed M-BFAS validated through fabrication and measurements.

2. BASIC DESIGN CONCEPT OF M-BFAS

The Butler matrix array is the most popular of all beam forming networks used to design a M-BFAS. The $N \times N$ Butler matrix network consists of N input and N output ports, where $N = 2^n$. The system requires $2^{n-1} \log_2 2^n$ and $(\frac{2^n}{2})[\{\log_2 2^n\} - 1]$ numbers of 3 dB coupler and 45° phase shifter respectively [16]. The crossover or 0 dB coupler is used in the path crossing of two transmission lines for the single layer implementation of Butler matrix array. A basic block diagram of 4×4 M-BFAS is shown in Figure 1.

The output ports of the Butler matrix array feed the antenna elements A_1, A_2, A_3 and A_4 as shown
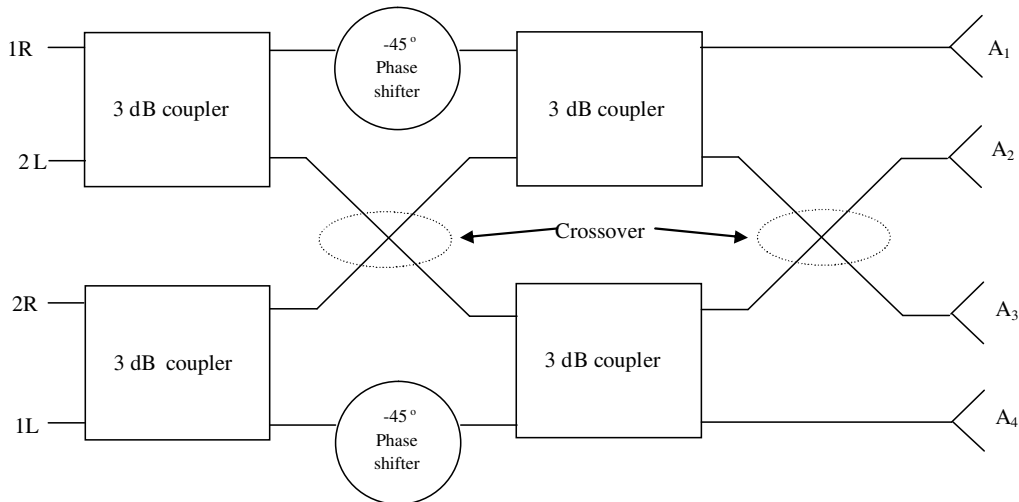
**Figure 1.** Basic block diagram of symmetric 4×4 multiple beam forming antenna system.

in Figure 1 to create the directive beams in the different directions. The input ports of the system are named as 1R, 2L, 2R and 1L based on the specific direction of the major beams (R: Right and L: Left). The 1R port excitation leads the system to generate the major directive beam in the range of 0° to 30°. Similarly remaining major beams directions should be in the range of −30° to −60°, 30° to 60° and 0° to −30° for 2L, 2R and 1L port excitation respectively. The pointing major beam directions for 4×4 beam forming antenna system can be calculated as follows [17]

$$\theta = \cos^{-1}\left[\frac{\pm (2n-1)\,\lambda_0}{8d}\right] \tag{1}$$

where $n = 1, 2, \ldots, \lambda_0$ is free space wavelength, and d the physical distance between the centers of antenna elements.

3. SUBSTRATE INTEGRATED WAVEGUIDE AND SUBSTRATE INTEGRATED FOLDED WAVEGUIDE TECHNOLOGY

SIW is the dielectric filled waveguide and can be integrated with the planar circuits and devices. The fabrication process of SIW in planar form accomplished by using periodic metallic via holes, air holes or
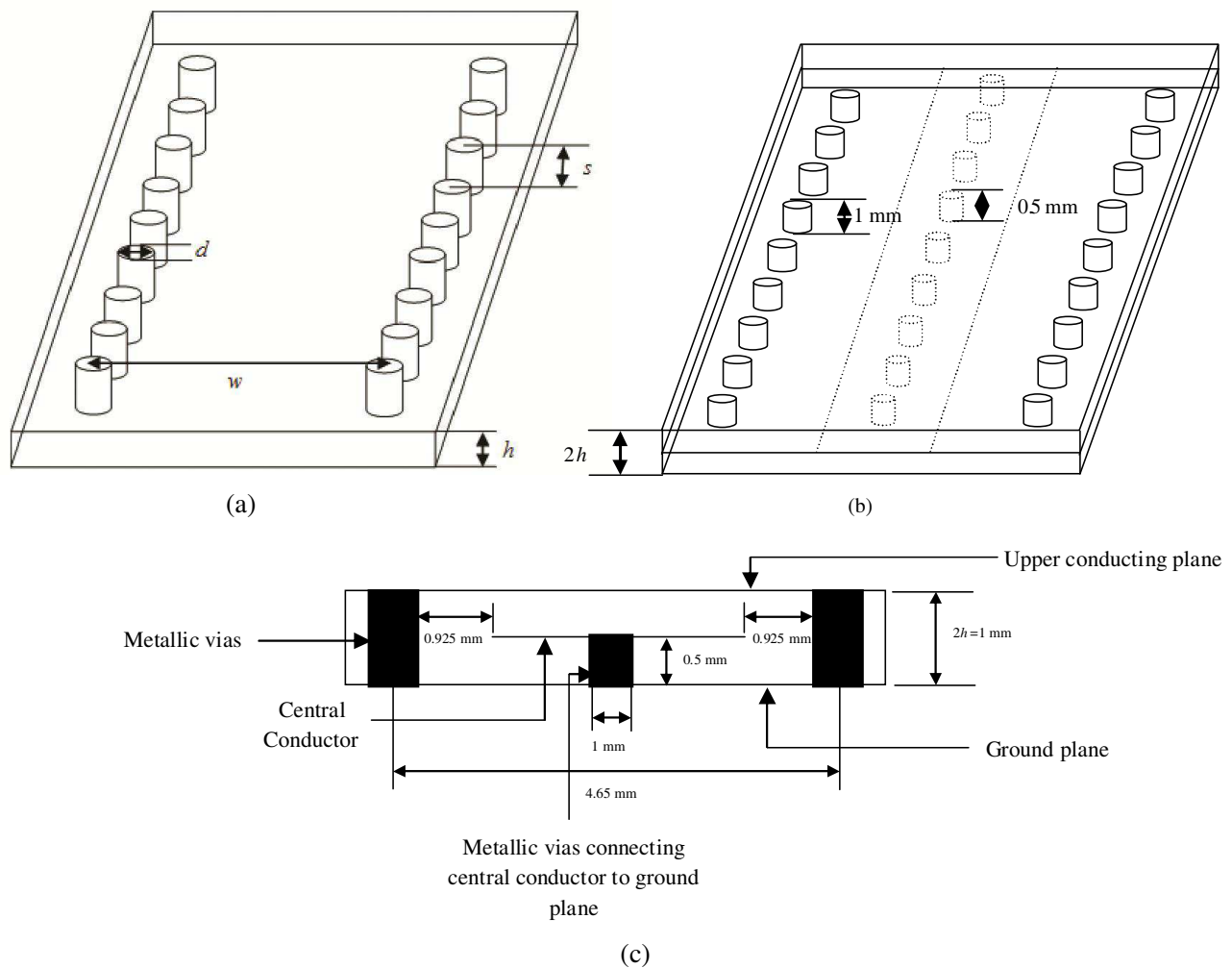

Figure 2. (a) Design of SIW with $w = 9.3\,\text{mm}$, $d = 1\,\text{mm}$, and $s = 2\,\text{mm}$. (b) Design of SIFW. (c) Cross sectional view of SIFW with $w = 4.65\,\text{mm}$ and $2h = 1\,\text{mm}$.

holes filled with different dielectric. The array of periodic metallic via holes is preferred over the other techniques for low leakage loss. The metallic pins shield the electromagnetic waves as well as connect the surface current in order to preserve the guided wave propagation. The width of SIW is calculated from the following equation [18]:

$$w_{eff} = w - 1.08\frac{d2}{s} + 0.1\frac{d2}{w} \tag{2}$$

where, d is the diameter of metallic pins, s the centre to centre distance between the vias, and w_{eff} the equivalent width of SIW. To use the above mentioned equation some conditions like $\frac{s}{d} < 2.5$ and $\frac{d}{w} < \frac{1}{5}$ should be maintained. The substrate integrated waveguide has been designed with $w = 9.3\,\text{mm}$, $d = 1\,\text{mm}$ and $s = 2\,\text{mm}$ for a cut-off frequency of $12\,\text{GHz}$. The planar implementation of rectangular waveguide using SIW technology reduces the width of waveguide by a factor of $1/\sqrt{\varepsilon_r}$, where ε_r is the relative permittivity of the substrate material. To reduce the width of SIW the substrate integrated folded waveguide (SIFW) technology has been chosen. It finally reduces the width of standard waveguide by a factor $1/(2\sqrt{\varepsilon_r})$ without affecting the cut-off frequency [19, 20]. The basic design of SIW and SIFW and a comparison of S-parameter characteristics of both the structures are shown in Figure 2 and Figure 3, respectively.
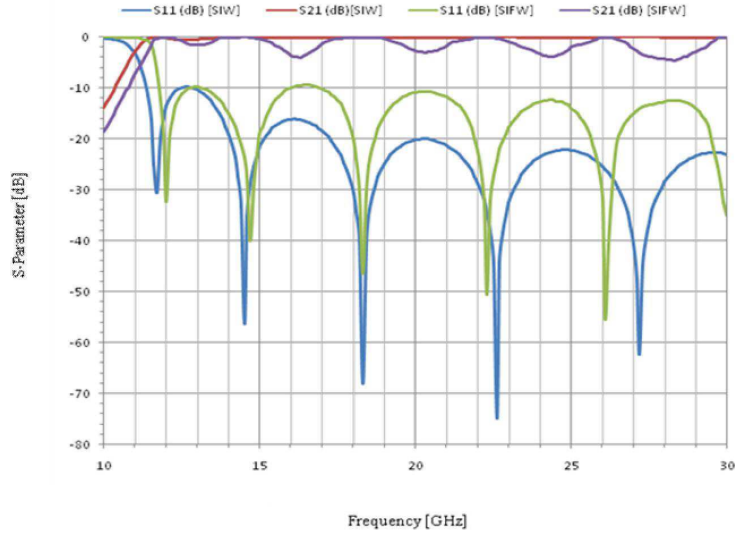

Figure 3. Comparison of S-parameter characteristics of SIW and SIFW.

The metallic vias connect the strip line of the middle layer to bottom layer as shown in Figure 2(b). Hence the bottom layer will act as the ground plane of strip line.

The designed SIW and SIFW are simulated, and the results are shown in Figure 3. It shows that the cut-off frequency has not changed for both the structures although the width of SIFW is exactly half the width of SIW, and also the performance is similar to the classical standard waveguide. Although the response of SIFW is slightly degraded with respect to SIW, the values of S_{11} ($-22.81\,\text{dB}$) and S_{21} ($-0.27\,\text{dB}$) at $14.9\,\text{GHz}$, which is the design frequency for the proposed antenna system are good.

4. SIFW H-PLANE 3 dB DOUBLE SLOT COUPLER

Rectangular waveguide coupler can be formed by using two individual waveguides, sharing the common broad wall [21]. Slots are introduced with a certain distance apart from each other in the common wall to couple the two waveguides. SIW technology can be used for planar implementation of waveguide 3 dB coupler and also for size reduction. Further size reduction can be achieved by using SIFW technique as it reduces the width of SIW by a factor 0.5. The 3 dB directional coupler consists of four ports as shown in Figure 4(a).
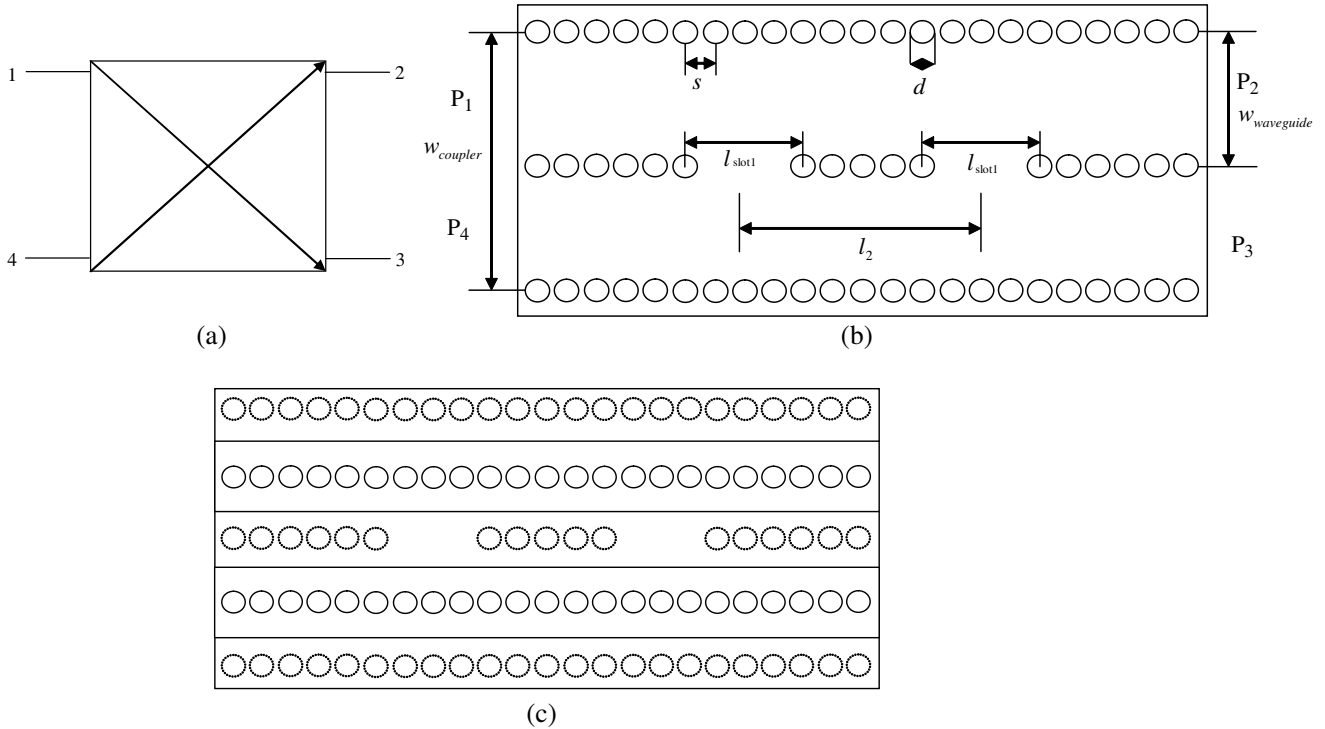
Figure 4. (a) Basic structure of 3 dB coupler. (b) Upper layer and (c) middle layer of proposed SIFW H-plane 3 dB double slot coupler.

Ports 1, 2, 3 and 4 are named as input, output, coupled and isolated port respectively. The input power should be divided equally in the ports 2 and 3 with 90° phase difference between them and port 4 should be isolated.

The proposed structure of SIFW H-plane 3 dB double slot coupler is shown in Figures 4(b) and 4(c).

The centre of the two slots should be at a distance of $(n - \frac{1}{2})\lambda_g$ {where $n = 1, 2, \ldots,$ etc. and λ_g is the guided wavelength}, to make the phase difference of coupled waves at these two slots equal to 180° at the port 4 and hence improve the isolation [22]. The design parameters are listed in Table 1.

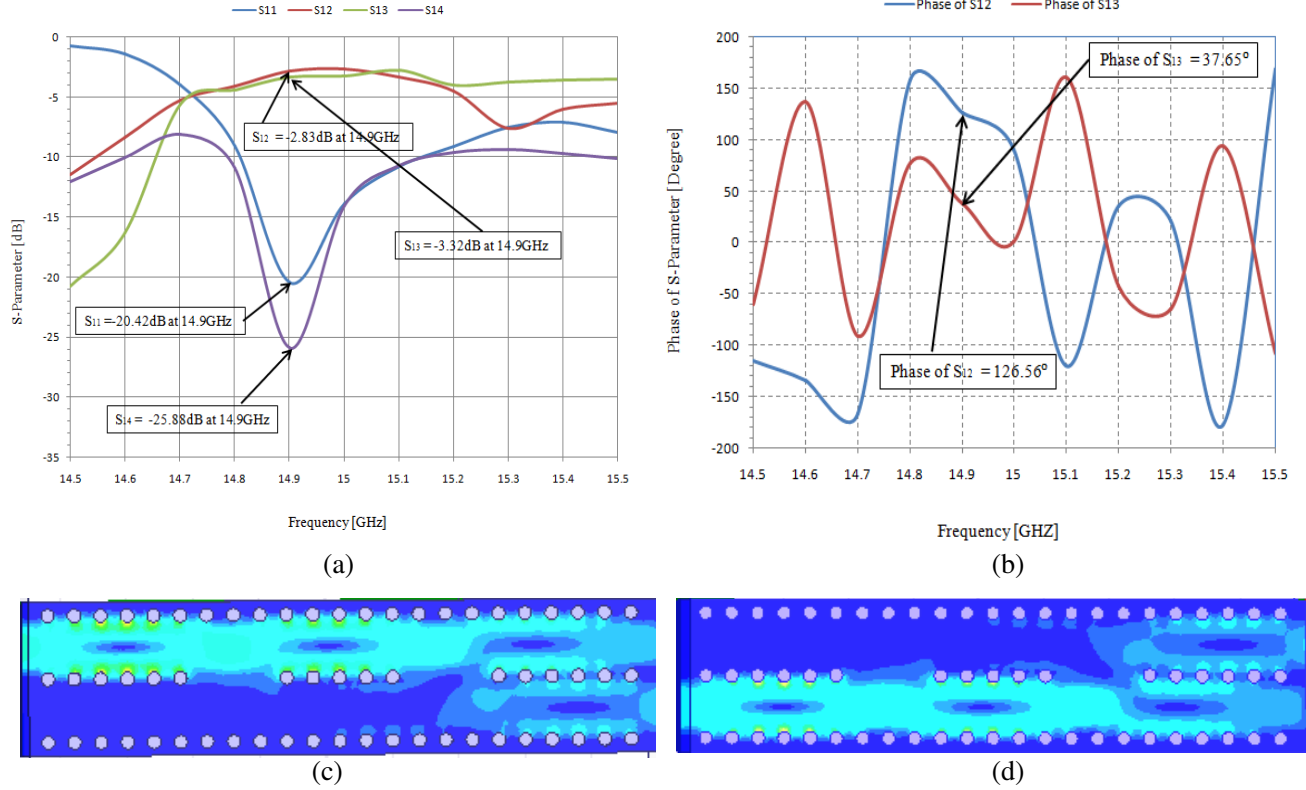**Table 1.** Design parameters of SIFW H-plane 3 dB double slot coupler.

Parameters	Unit (mm)
s	2
d	1
l_{slot1}	8
l_2	16
$w_{waveguide}$	4.65
$w_{coupler}$	9.3

The optimized slot length to get 3 dB coupling is 8 mm and considerably smaller than the couplers proposed in previous papers and also the overall length of the coupler is reduced [22–24]. A comparison of total length of proposed and previously designed 3 dB double slot coupler is given in Table 2.

The designed coupler is simulated and the characteristics are measured using wave port feeding technique at the inputs and outputs. The simulated reflection loss (S_{11}), transmission coefficient (S_{12}),

Table 2. Comparison between total length of proposed and previously developed 3 dB double slot coupler.

| Total length of Proposed coupler [mm]	Total length [mm]		
	Reference [22]	Reference [23]	Reference [24]
48	52.8	54.4	69.7
Size reduction in %	9.1%	11.76%	31.13%

Figure 5. Simulation results of SIFW H-plane 3 dB double slot coupler: (a) Magnitude of S-parameter characteristics; (b) Phase of transmitted and coupled signal; (c) Current distribution for 1st port and (d) 4th port excitation.

coupling (S_{13}) and isolation (S_{14}) level of the SIFW H-plane 3 dB double slot coupler are at -20.42 dB, -2.82 dB, -3.32 dB and -25.88 dB at 14.9 GHz respectively as illustrated in Figure 5(a). The phase difference of $88.91°$ has been achieved between the output ports of the coupler as shown in Figure 5(b). A bandwidth of 330 MHz has been achieved considering -10 dB S_{11} value as cut off as shown in Figure 5(a). It is observed from Figure 5(b) that the phase difference between the two output ports remains stable (approximately 90°) for the frequency bandwidth of 170 MHz starting from 14.82 GHz to 14.99 GHz. The current distribution at 14.9 GHz for the 1st port excitation is observed in Figure 5(c), and it is clear from the figure that a good isolation level has been achieved at port 4. The reverse happens if the excitation is given in port 4 (Figure 5(d)) and hence proved the symmetricity of the structure. The directivity of the coupler depends upon the number of coupling slots. For a single slot coupler the directivity bandwidth is comparatively low. To improve the bandwidth of directivity it is necessary to increase the number of slots. The double slot coupler is a suitable option for the proposed BFN as it will provide good directivity over the entire frequency band (330 MHz) as shown in Figure 5(a). Also the use of two coupling slots introduces a degree of freedom to control the coupling level of the coupler [22].

5. SIFW H-PLANE 0 dB DOUBLE SLOT COUPLER (CROSSOVER)

The four-port terminal directs the power from input port 1 to coupled port 3, and the remaining ports (port 2 and port 4) are in isolation. The operation is altered if the signal is given to port 4. The conventional 0 dB coupler is formed by cascading two 3 dB couplers back to back and it is shown in Figure 6 [12].
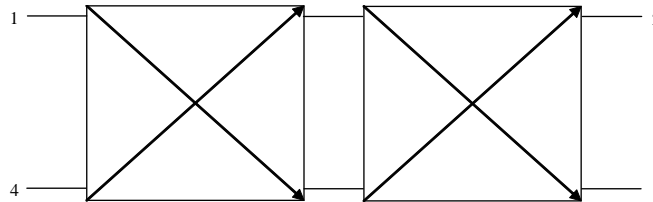

Figure 6. Basic structure of 0 dB coupler.

The coupling level can be controlled by varying the coupling slots lengths. The SIFW H-plane 0 dB coupler is formed by changing the parameters l_{slot1} and l_2 of the 3 dB coupler [23, 25]. This technique makes the volume of 0 dB coupler identical to the single 3 dB coupler as well as reduces the length by 50%. Hence, the additional volume of conventional design is decreased. The proposed 0 dB coupler is presented in Figure 7.


(a)

(b)
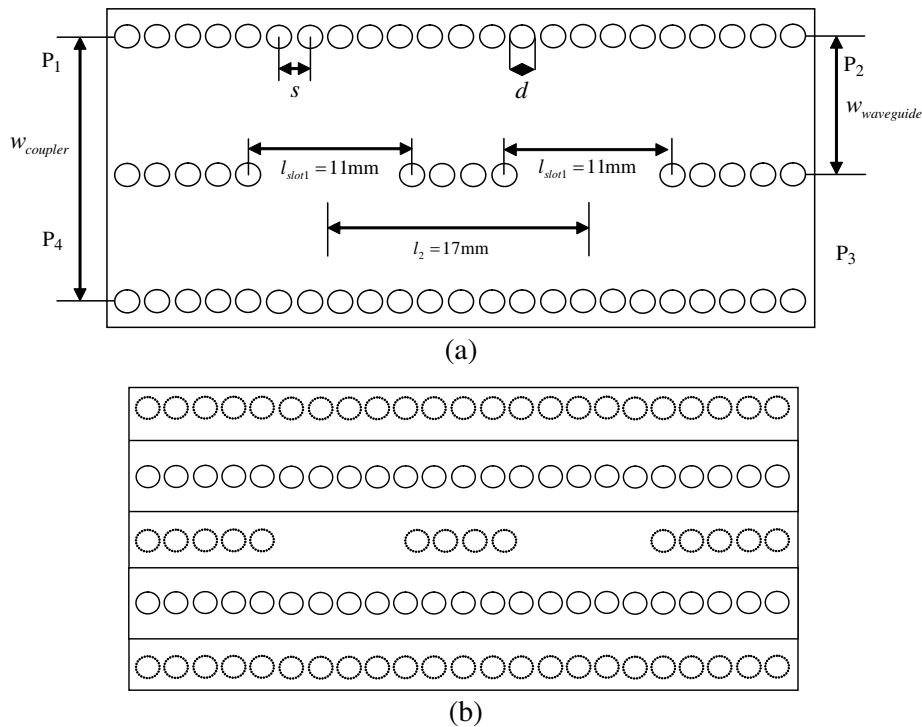
Figure 7. (a) Upper layer and (b) middle layer of proposed 0 dB coupler.

The reflection loss (S_{11}) and coupling level (S_{13}) of -20.16 dB and -0.13 dB have been achieved in simulation as shown in Figure 8(a). The approximate frequency bandwidth of 170 MHz has been obtained using similar criterion over -10 dB of S_{11}. For calculating the bandwidth for S_{13}, -1.5 dB has been considered as the threshold so that at least 75% of the input power travels to the output. The coupling level (S_{13}) better than -1.5 dB has been achieved over the range of 120 MHz (14.88–15 GHz).

(a)

(b)   (c)
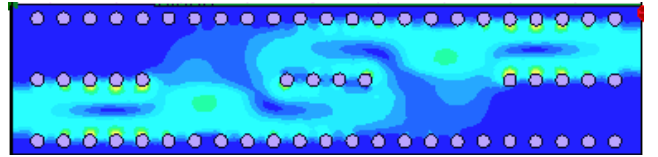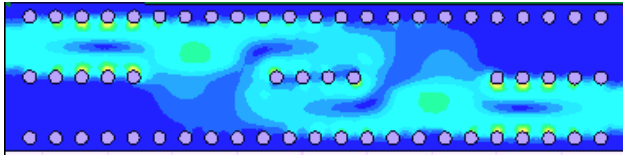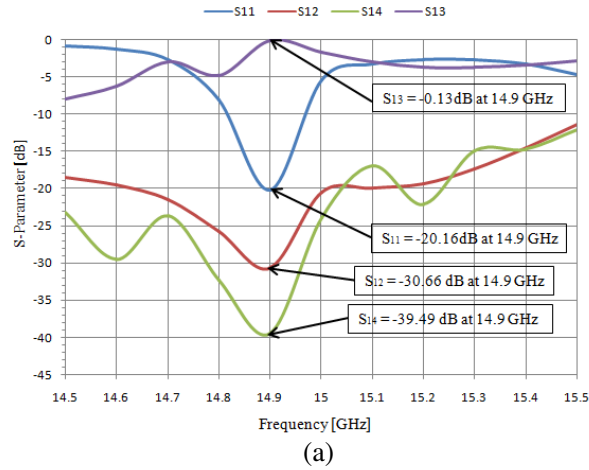
Figure 8. Simulation results of SIFW H-plane 0 dB double slot coupler: (a) Magnitude of S-parameter characteristics; (b) Current distribution for 1st port and (c) 4th port excitation.

(a)   (b)
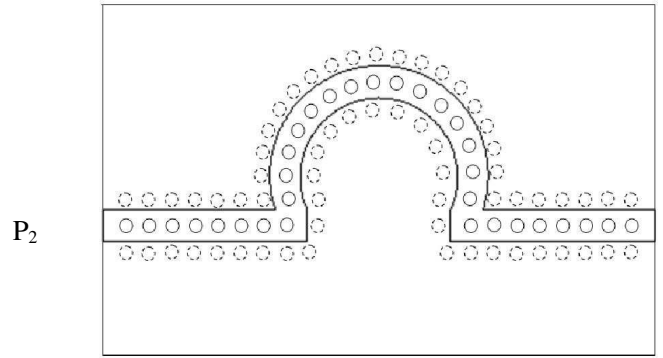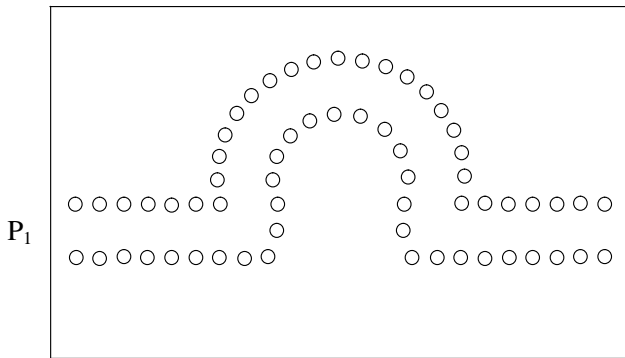
Figure 9. (a) Upper layer and (b) middle layer of proposed SIFW 45° phase shifter.

At the design frequency (14.9 GHz), most of the power with minimum loss ($S_{13} = -0.13$ dB) is coupled to port 3 which is the basic need. A maximum loss of -1.5 dB is observed at 14.88 GHz and 15 GHz within the operational bandwidth. The bandwidth of directivity depends upon the number of coupling slots, in the proposed design only two coupling slots have been used similar to 3 dB coupler to reduce the length of the crossover. More number of series slots will improve the value of S_{13} over the entire band (170 MHz). But the use of multiple slots will increase the length of crossover. A compromise had to be done to get good performance without increasing the length. Good isolation has been achieved for port 2 ($S_{12} = -30.66$ dB) and port 4 ($S_{14} = -39.49$ dB) and it is validated by the current distribution of the 0 dB coupler as shown in Figure 8(b). The operational property of a 0 dB coupler is inverted if the signal is fed to port 4 and it is clearly visible in Figure 8(c) proving the design symmetricity.
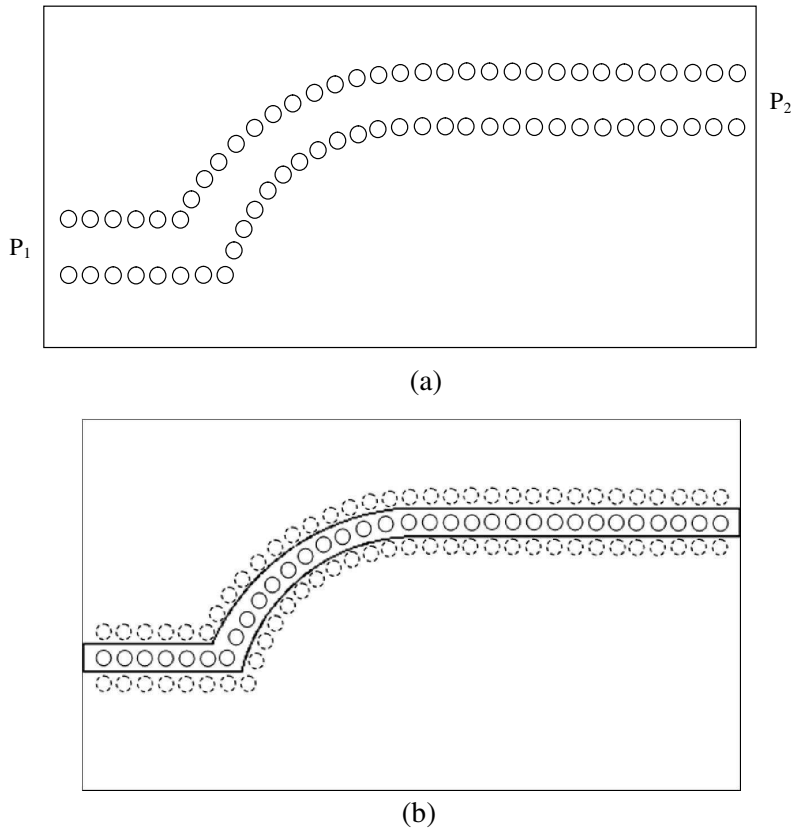
6. SIFW 45° AND 0° PHASE SHIFTER

The 45° phase shifter is a key component of M-BFN. It is realized by the SIFW technology as shown in Figure 9.

The output ports of the Butler matrix network should be aligned properly to integrate the antenna elements with the specified centre to centre distance between them as stated in Section 2. The curved transmission lines have been used for the appropriate alignments of the output ports, so that can easily be attached with the antenna array by maintaining the physical distance d between the radiating elements. Ideally, the phase delay provided by the curved SIW transmission line should be 0°. The proposed structures are given in Figure 10 and Figure 11, respectively.

A phase shift of −46.82° has been attained at 14.9 GHz by the proposed phase shifter as shown in Figure 12(a). From Figure 12(b) it can be observed that the reflection loss (S_{11}) and transmission coefficient (S_{12}) of −21.99 dB and −0.191 dB respectively have been achieved. The current distribution has been shown in Figure 12(c), showing almost lossless flow of current.

Satisfactory S-parameter characteristics are observed in Figure 13(a) for the 0° phase shifter. A 0° phase shift is quite difficult to achieve practically due to its path length. The proposed design provides a phase shift of −6° as shown in Figure 13(b). Figure 13(c) shows the current distribution.

The simulated S-parameter characteristics are reported in the Figure 14(a) and it is observed that a satisfactory performance has been achieved. A phase shift of −1.74° has been achieved as shown in Figure 14(b). This design shows better response than the previously designed 0° phase shifter because of the reduced path length for the traveling wave to reach the output. Figure 14(c) shows the current distribution of the proposed SIFW 0° phase shifter.

(a)

(b)

Figure 10. (a) Upper layer and (b) middle layer of proposed SIFW 0° phase shifter.
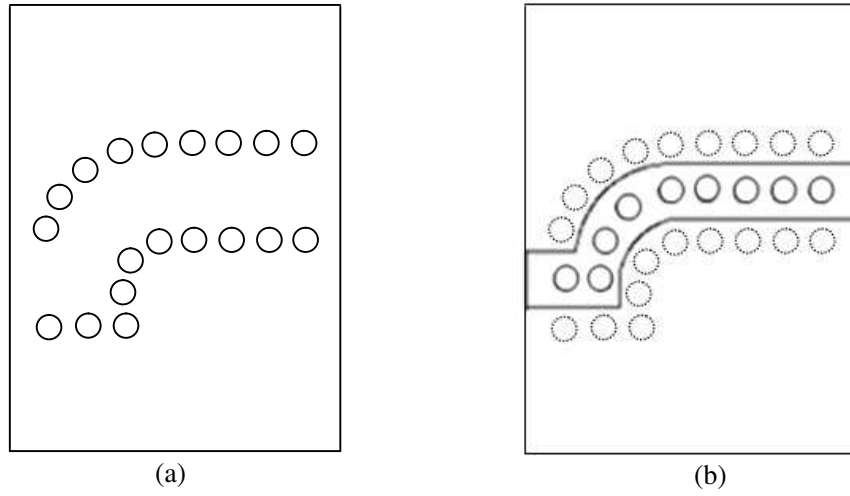
(a)

(b)

Figure 11. (a) Upper layer and (b) middle layer of proposed SIFW 0° phase shifter.
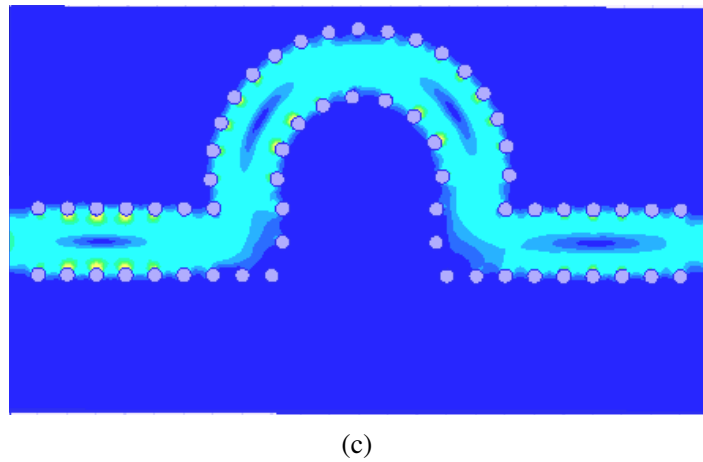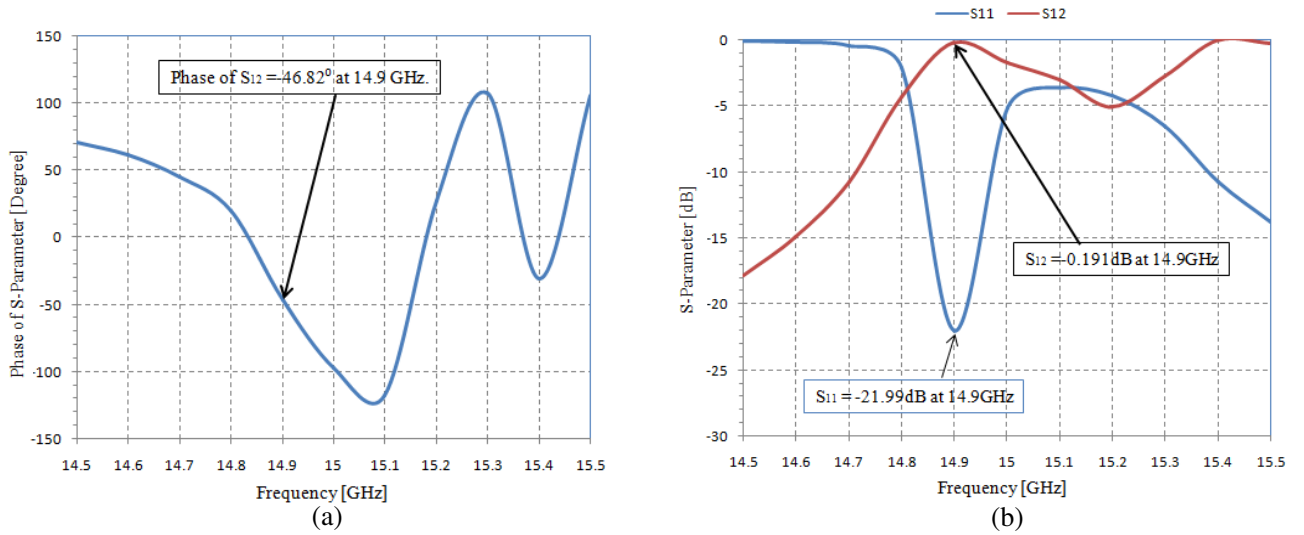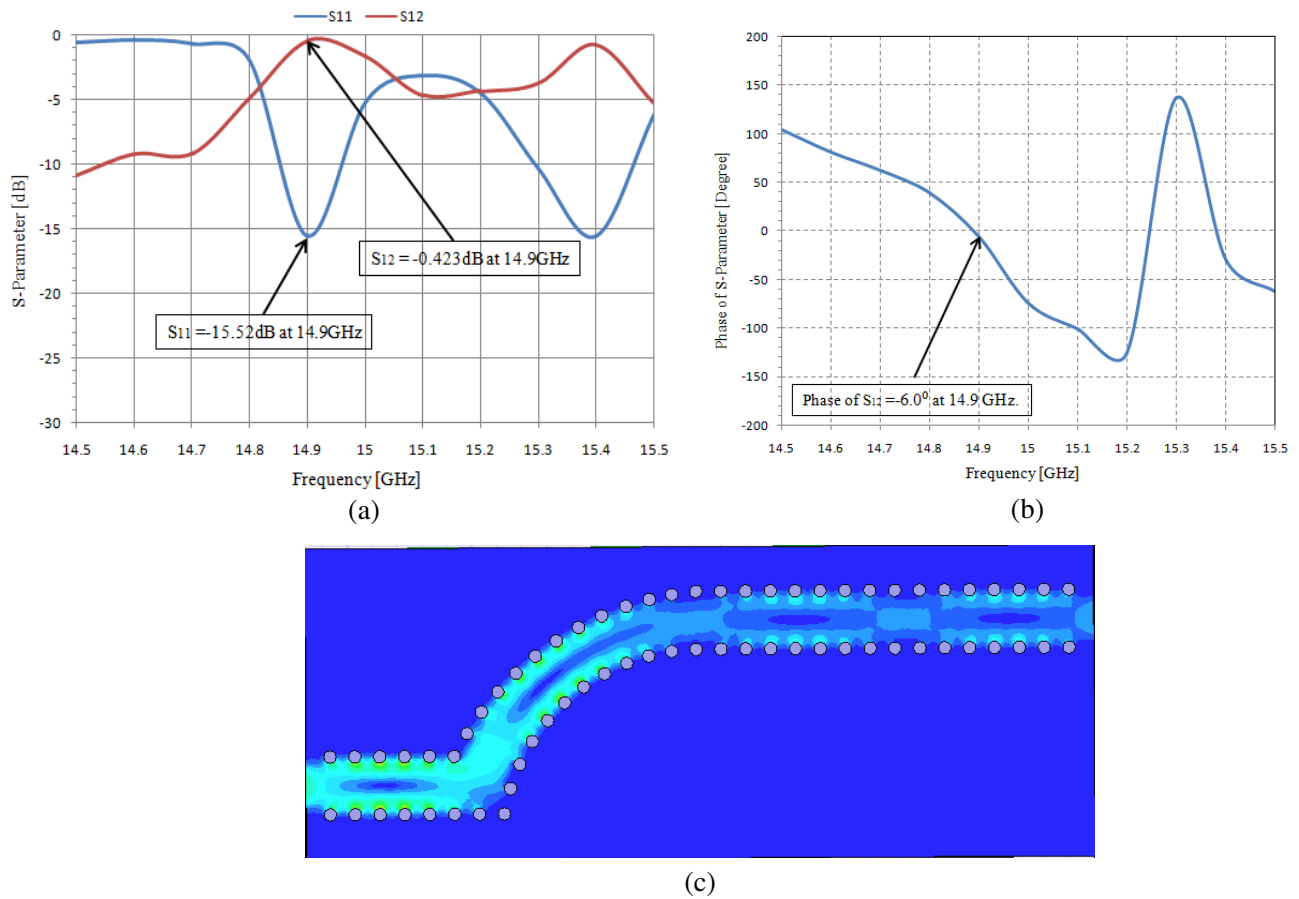

(a)

(b)

(c)

Figure 12. Simulation results of SIFW 45° phase shifter: (a) Phase difference between the input and output ports; (b) Magnitude of S-parameter characteristics and (c) current distribution.
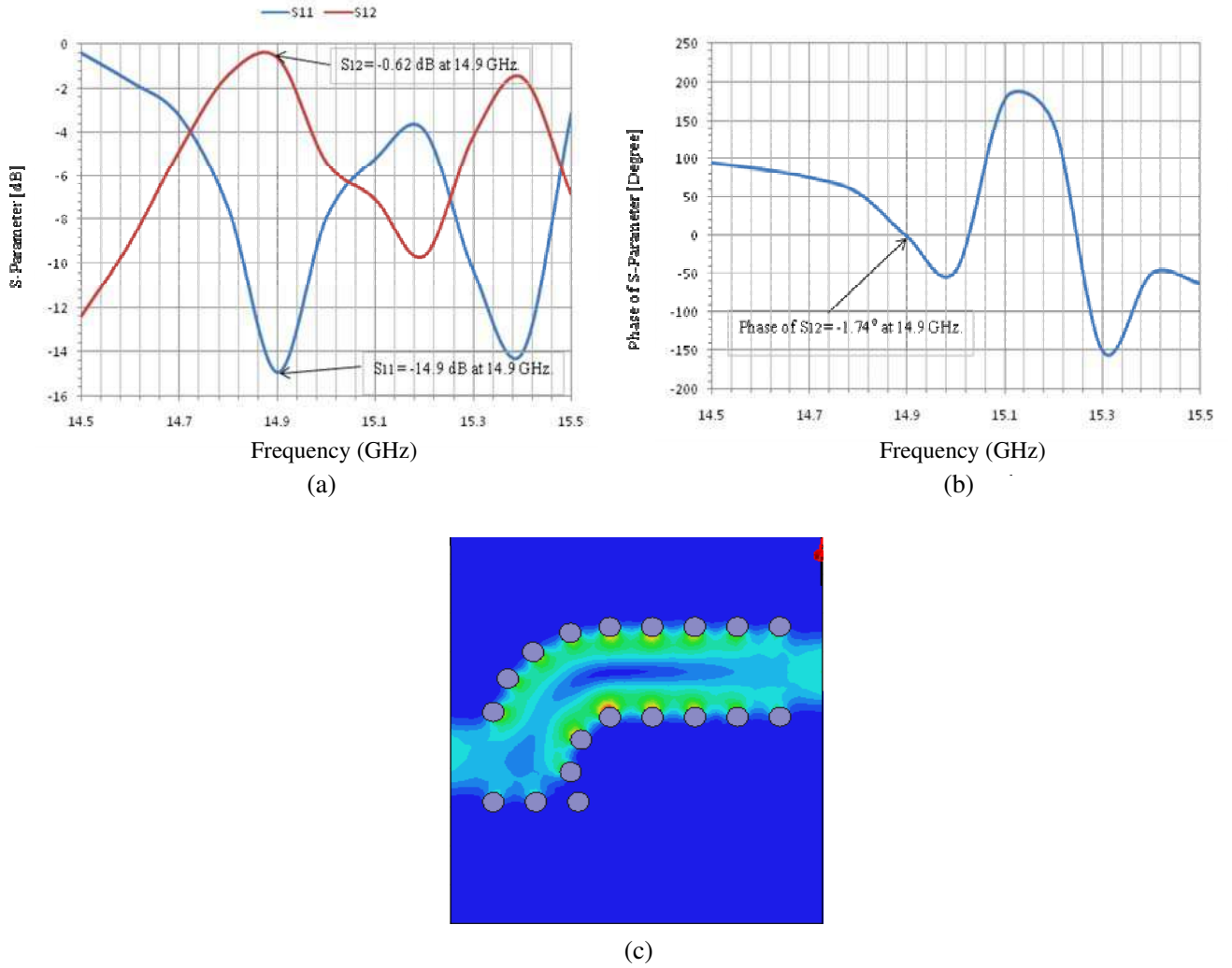
(a)

(b)

(c)

Figure 13. Simulation results of SIFW $0°$ phase shifter: (a) Magnitude of S-parameter characteristics; (b) Phase difference between the input and output ports and (c) current distribution.

7. COMPLETE STRUCTURE OF PROPOSED SIFW BUTLER MATRIX ARRAY

The basic building blocks of Butler matrix array have been developed by using SIFW technology. The simulation results of these key components are quite satisfactory as reported in the previous sections. The formation of the proposed Butler matrix array involves a combination of these key components leading to convincing performance of the system at the frequency of interest. Design of upper and middle layer of the proposed SIFW Butler matrix array is presented in Figures 15(a) and 15(b) respectively.

The implementation of the waveguide coupler has been done by using slots at the common wall of the two waveguides and it makes the coupler more compact in width as well as reduction in width of the whole BFN. The length of the coupler is slightly more due to use of two slots to improve the isolation level at port 4 and directivity bandwidth. In [12] the cruciform couplers are incorporated in Butler matrix array increasing the width of the matrix. In the proposed design, the coupler is formed by SIFW and common wall technique which reduces the width of complete Butler matrix array. Also for the implementation of larger matrices such as 8×8 or 16×16, the proposed design can easily be used maintaining the compactness in width. The width of Butler matrix array is 45.83 mm as shown in Figure 15(a). An approximate width reduction of 50% and 41% has been achieved as compared to the previous designs described in [12, 14] respectively. Thus the SIFW technique also makes the fabrication process simpler. The simulation results of proposed BFN are given in Figure 16.

Adequate matching is achieved for all the ports of proposed Butler matrix array. The reflection losses (S_{11}, S_{22}, S_{33} and S_{44}) of -15.7 dB, -19.67 dB, -24.7 dB and -17.64 dB have been achieved respectively as shown in Figure 16(a) at 15 GHz. Figures 16(b) and 16(c) represent the transmission

(a)

(b)

(c)

Figure 14. Simulation results of SIFW $0°$ phase shifter: (a) Magnitude of S-parameter characteristics; (b) Phase difference between input and output ports; (c) Current distribution.

coefficients of the Butler matrix array for 1st and 2nd port excitation respectively and it is observed that average power coupling level to the output ports is -7.5 dB for both port excitations. The symmetricity in Butler matrix array makes the system performance for the 3rd and 4th port excitation similar to the 2nd and 1st port excitation respectively. The isolation level between the input ports of Butler matrix array are well below -20 dB as reported in Figures 16(d) and 16(e). The phase differences between the output ports of the proposed Butler matrix array are listed in Table 3.

Table 3. Phase differences between the output ports of the proposed Butler matrix array for 1st and 2nd port feeding.

	Port Excitation	Phase differences between output ports		
		$S_{15} - S_{16}$	$S_{16} - S_{17}$	$S_{17} - S_{18}$
At 15 GHz	1	$123.6°$	$123.67°$	$126.87°$
	2	$S_{25} - S_{26}$	$S_{26} - S_{27}$	$S_{27} - S_{28}$
		$-39.4°$	$-36°$	$-35.75°$

(a)

(b)
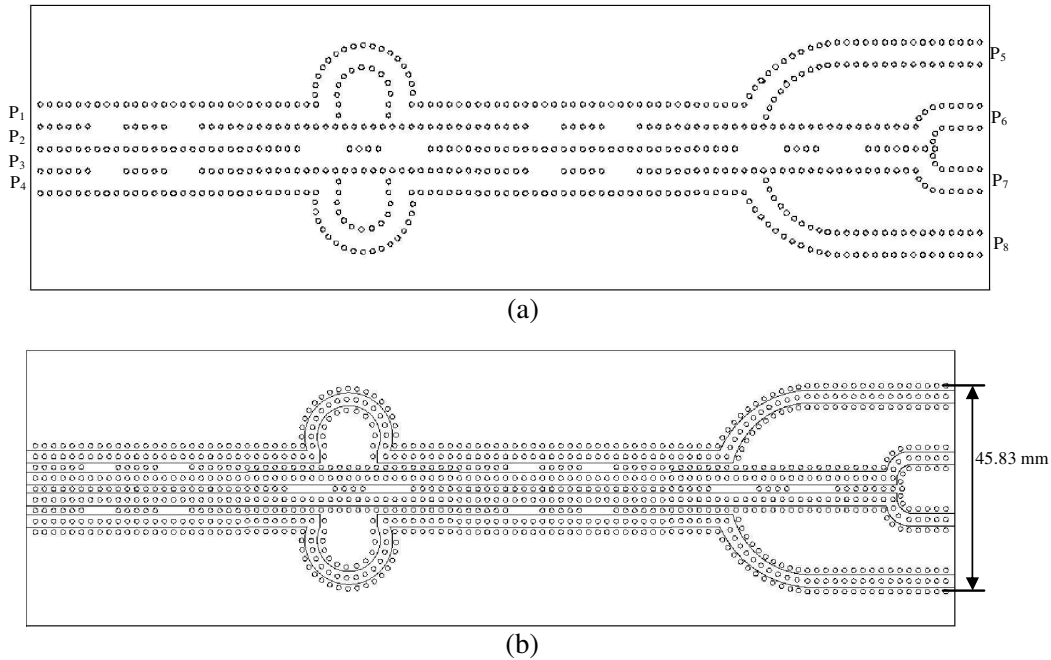
**Figure 15.** (a) Upper layer and (b) middle layer of the proposed SIFW Butler matrix network.

From the above discussions, it is clear that a satisfactory performance for the proposed Butler matrix array has been achieved at 15 GHz. The resonant frequency shifts by 0.1 GHz when all the components are combined to form the Butler matrix. As the wave traveling from the input port to the output port is coupled several times and some of the path length is common between the individual elements leading to reduction in total path traveled. This might be the reason for the shift of 0.1 GHz in the resonance frequency of the complete structure.

8. SIFW H-PLANE HORN ANTENNA

An SIFW H-plane horn antenna has been developed as the radiating element and it is fed by the output ports of proposed M-BFN to create the directive beams. The volume of H-plane SIW horn antenna [26, 27] is reduced by using the SIFW technology. The geometry of upper and middle layer of proposed horn antenna are shown in Figures 17(a) and 17(b) respectively.

Generally, the aperture dimension of the horn is high, as in [27] the length of the aperture is 14 mm for the resonant frequency of 27 GHz. This paper describes the design of H-plane horn antenna whose aperture length is 11.9 mm for the resonant frequency 15 GHz as shown in Figure 17(a). Considerable reduction in total volume of the antenna is achieved by reduction in aperture length although the height has increased two times for a frequency 12 GHz lower than the previously reported design.

The performance of the SIFW Butler matrix array is good at 15 GHz as observed in the previous section, hence the H-plane SIFW horn antenna is designed for the frequency of 15 GHz for the best performance of the M-BFAS. The simulated reflection loss of -20.1 dB has been achieved at 15 GHz as shown in Figure 18(a). Figure 18(b) shows the plot of gain with respect to theta (θ) at 15 GHz. A gain of 2.7 dB is obtained at 0°. Radiation pattern shows a significant amount of back radiation. This may be a result of reduction in the aperture length of the horn for compactness of the complete structure. In the next section it would be observed that this back radiation does not have any negative impact on the radiation performance of the complete proposed MBFAS. The current distribution of the antenna at 15 GHz is reported in Figure 18(c). A satisfactory performance is obtained by the proposed antenna and is used as the radiating element in M-BFAS to generate the directive beams in the different directions. The radiation performance of the proposed M-BFAS is explained in the next section.
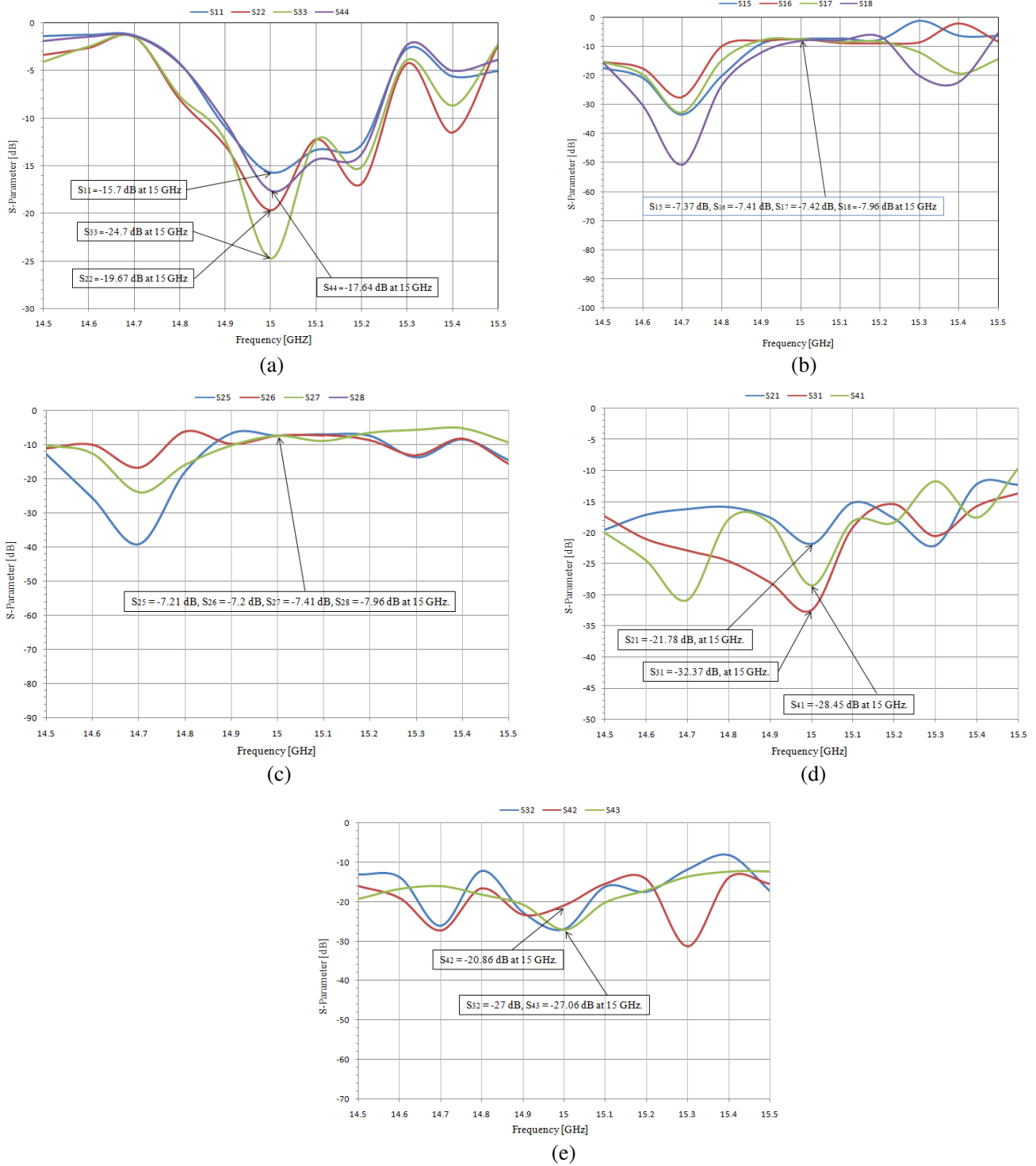
Figure 16. Simulation results of proposed SIFW Butler matrix array: (a) Reflection loss for different port excitations; (b) Transmission coefficients for 1st port excitation; (c) Transmission coefficients for 2nd port excitation; (d) and (e) Isolation between the input ports.

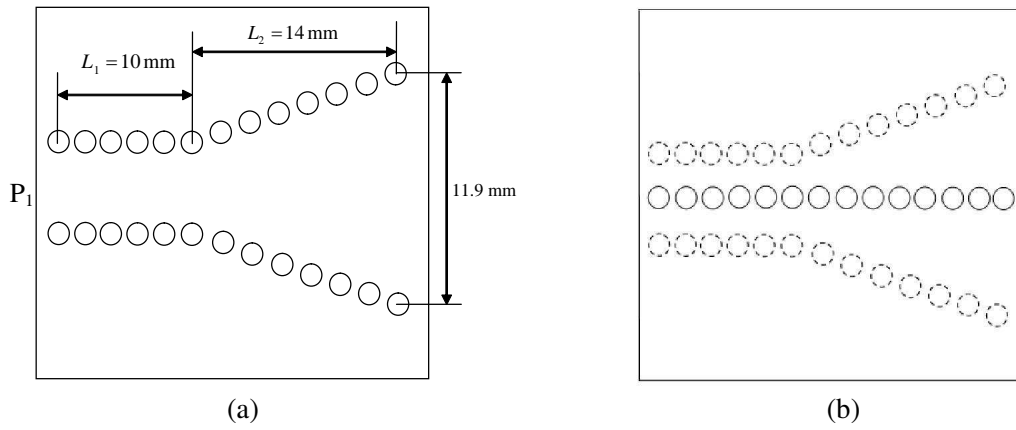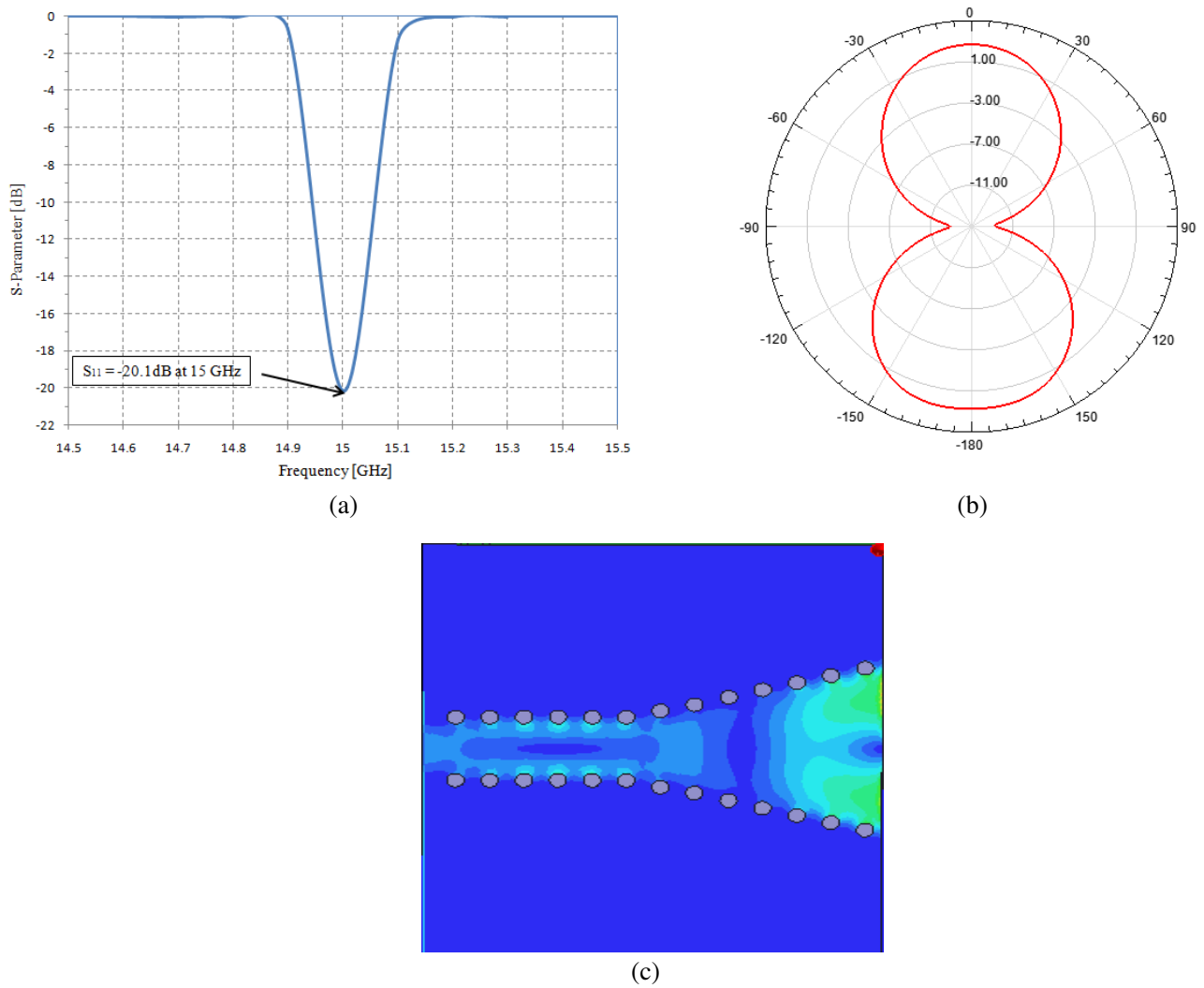**Figure 17.** Proposed SIFW H-plane horn antenna: (a) Upper and (b) middle layer.

Figure 18. Simulation results of proposed SIFW H-plane horn antenna: (a) Reflection loss (S_{11}); (b) H-plane radiation pattern and (c) current distribution.

9. SIFW MULTIPLE BEAM FORMING ANTENNA SYSTEM (SIFW M-BFAS)

This section presents the complete design of SIFW M-BFAS as proposed in this paper. All the individual components along with Butler matrix array and horn antenna have been designed. Finally the whole M-BFAS has been developed and realized practically. The layout and fabricated structure of SIFW M-BFAS are presented in Figure 19.

Initially, the middle layer of the proposed structure (shown in Figure 19(b)) was fabricated, all the necessary drillings have been accomplished and the holes are filled with metal pins as shown in

(a)

(b)

(c)

(d)
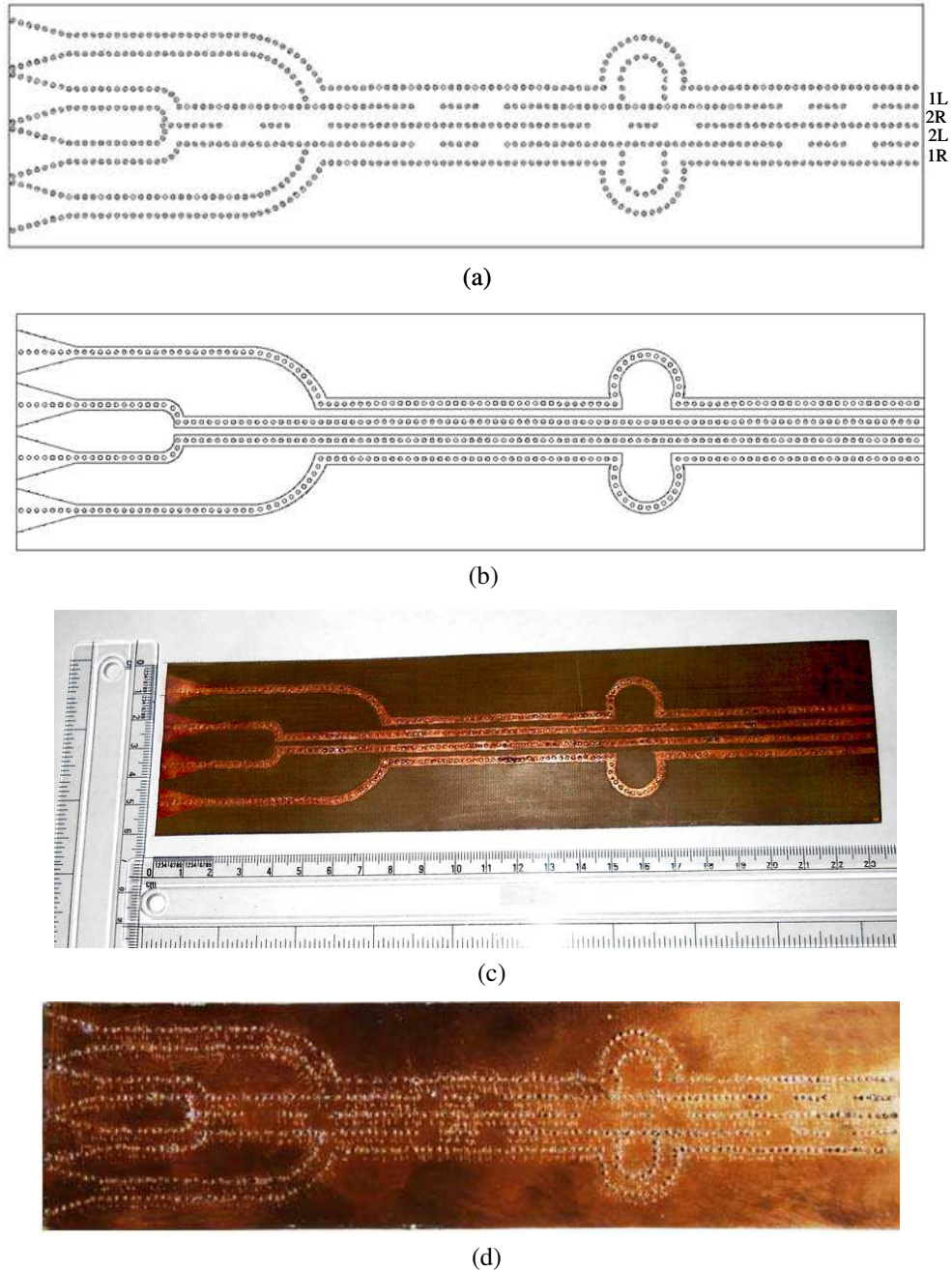
Figure 19. Layout and fabricated structure of proposed SIFW M-BFAS: (a) Architecture of upper layer; (b) Architecture of middle layer and (c) fabricated structure of middle layer; (d) Fabricated structure of whole SIFW M-BFAS.
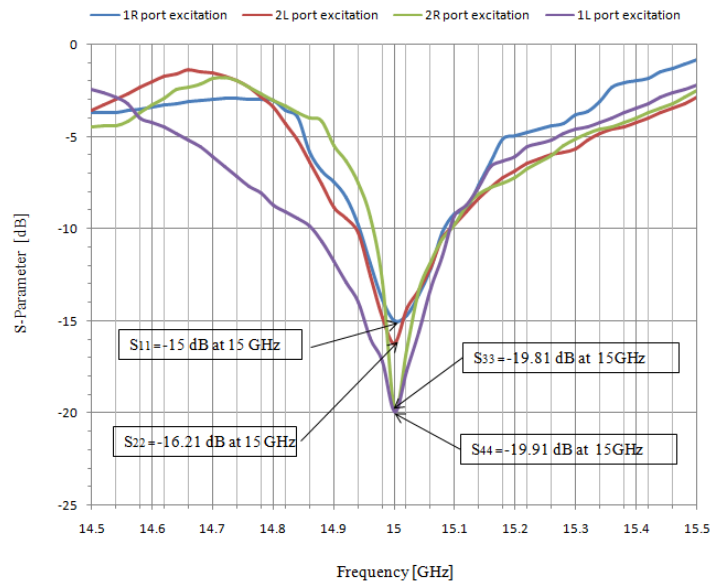
Figure 20. Measured reflection losses for different port excitation.

Figure 19(c). Figure 19(a) presents the upper layer of M-BFAS. The fabrication of upper layer is done individually, and then it is placed on the middle layer. All the drillings are done from the upper layer through middle layer to ground plane, metallic pins are inserted in the holes to create the electrical walls so that the electromagnetic wave does not leak and also provides a guided path from input to output. The alignment between the two layers is maintained so that the metallic pins inserted from upper layer to ground plane do not interfere with the conducting plane of middle layer. The fabricated SIFW M-BFAS is depicted in Figure 19(d).

The measurements of proposed SIFW M-BFAS have been carried out using Agilent N5230A PNA-L network analyzer, signal generator (SMR20, 1 GHz–20 GHz) and spectrum analyzer (FSP, 9 kHz–30 GHz). The measured reflection losses for different port excitations are presented in Figure 18. In measurements good matching ($S_{11} = -15$ dB, $S_{22} = -16.21$ dB, $S_{33} = -19.81$ dB and $S_{44} = -19.91$ dB) has been achieved at 15 GHz as shown in Figure 20. Figures 21(a), 21(b), 21(c) and 21(d) depict the simulated and measured normalized radiation patterns at 15 GHz for 1R, 2L, 2R and 1L port excitation respectively. Good directive beams have been achieved both in simulations and measurements by the proposed structure as shown in Figure 21. The side lobe levels are well below -18 dB both in simulations and measurements. The aperture size of proposed H-plane SIFW horn antenna is very less and getting good directive beams by integrating this proposed horn antenna with the SIFW Butler matrix array can be considered as a major achievement. So for the larger M-BFAS such as 8×8 or 16×16, this compact H-plane SIFW horn antenna can easily be accommodated by providing the specific inter elements spacing between them and will generate more directive beams.

The comparison between calculated, simulated and measured beam directions is reported in Table 4. The beam directions are calculated by using Equation (1). The simulated and measured beam directions are in good agreement with the calculated results. The directivity and gain values of different beams

Table 4. Comparison between calculated, simulated and measured beam directions.

Beams	Calculated	Simulated	Measured
1R	$10.75°$	$10°$	$10°$
2L	$-34.03°$	$-32°$	$-34°$
2R	$34.03°$	$32°$	$34°$
1L	$-10.75°$	$-12°$	$-10°$
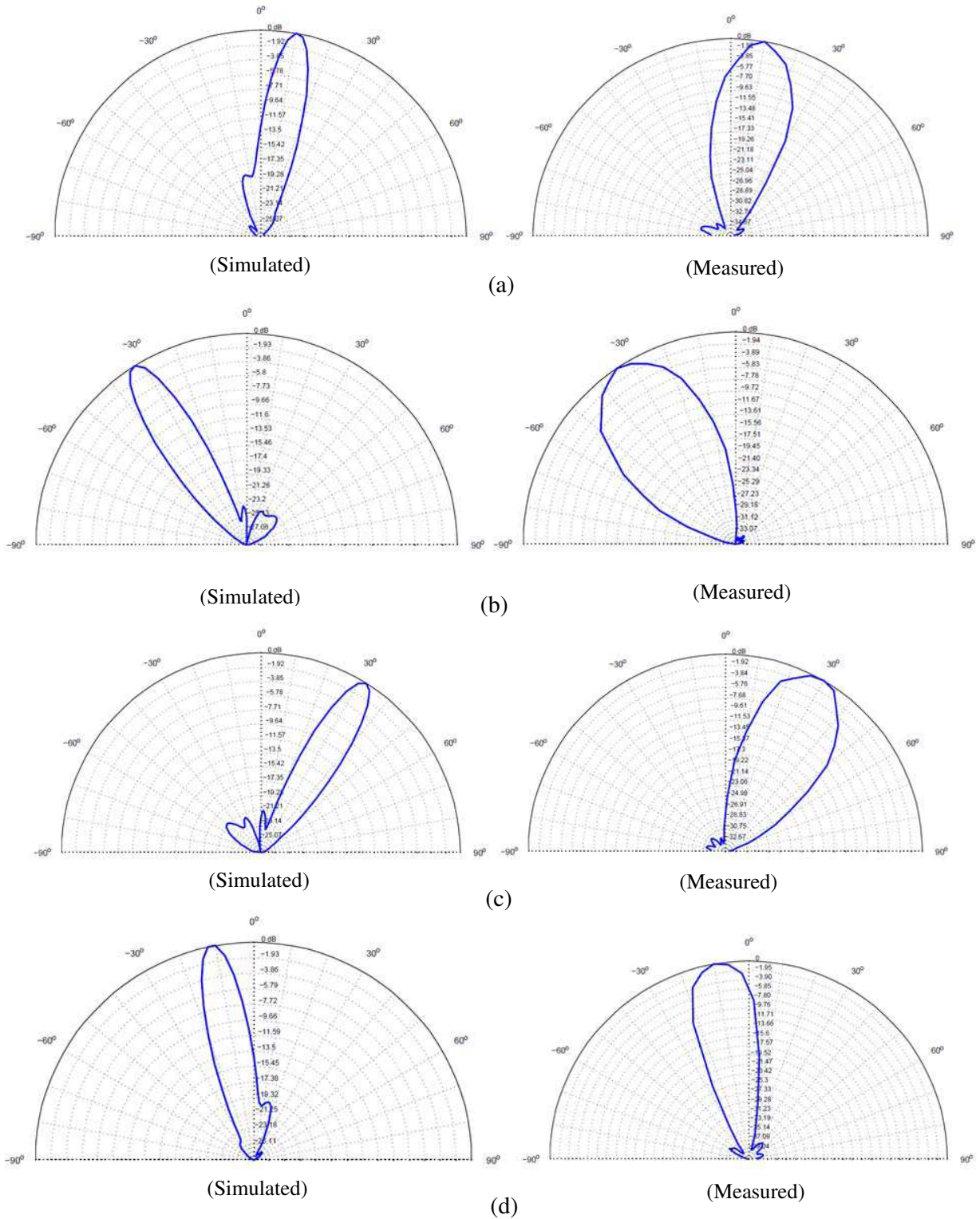
Figure 21. Simulated and measured normalized radiation pattern for different port excitation at 15 GHz: (a) Simulated and measured pattern for 1R port excitation; (b) Simulated and measured pattern for 2L port excitation; (c) Simulated and measured pattern for 2R port excitation and (d) simulated and measured pattern for 1L port excitation.

Table 5. Directivity and gain at 15 GHz for different beams.

Beams	Directivity (dB)	Gain (dB)
1R	6.41	5.8
2L	6.3	5.63
2R	6.23	5.31
1L	6.5	5.9

are reported in Table 5. The directivity of 6.41 dB, 6.3 dB, 6.23 dB and 6.5 dB and the gain of 5.8 dB, 5.63 dB, 5.31 dB and 5.9 dB for the beams 1R, 2L, 2R and 1L have been attained respectively at 15 GHz. The gain and directivity values are almost symmetric which is a requirement for the MBFAS. After going through the detail simulations and measurements it can be said that a good radiation performance have been achieved by the proposed M-BFAS.

10. CONCLUSIONS

The novel design of substrate integrated folded waveguide multiple beam forming antenna system (SIFW M-BFAS) has been described in this paper. All the necessary individual building blocks have been designed using SIFW technology. This technique reduces the width of SIW by half, and the same is applicable to the individual components. The common wall concept has been adopted to develop the 3 dB and 0 dB couplers. The dimensions of the 3 dB coupler have been reduced compared to the mostly available structures in literature. 0 dB coupling has been achieved by varying the coupling slots length of the same 3 dB coupler rather than using two 3 dB couplers in cascade form. Hence 50% length reduction has been achieved in 0 dB coupler. The aperture size of the horn antenna for the specific frequency application is reduced by using SIFW technology. All the individual building blocks are integrated to make the proposed Butler matrix array. The total width of BFN is reduced approximately by 50% and 41% as compared to the previously described designs. The length of system is slightly more than some of the earlier designs due to the use of double slot coupler, but reducing the width increases the possibility of integration of bigger matrices in a smaller area. Relative to the length of available double slot couplers, the proposed design is lesser in length. The performance of the proposed Butler matrix array or BFN is quite good.

Finally the M-BFAS has been developed by integrating the SIFW *H*-plane horn antenna with the proposed BFN. The radiation performance of the system shows that orthogonal beams are achieved. The simulation and measured normalized radiation performances are in good agreement. Besides these advantages the system is also less expensive and easy to realize.

REFERENCES

1. EI Zooghby, A., "Potentials of smart antennas in CDMA systems and uplink improvements," *IEEE Antennas and Propagation Magazine*, Vol. 43, No. 5, 172–177, Oct. 2001.
2. Blass, J., "Multi-directional antenna: New approach top stacked beams," *IRE International Convention Record*, Vol. 8, Part 1, 48–50, Mar. 1960.
3. Rotman, W. and R. Tuner, "Wide-angle microwave lens for line source applications," *IEEE Transactions on Antennas and Propagation*, Vol. 11, No. 6, 623–632, Nov. 1963.
4. Butler, J. and R. Lowe, "Beam-forming matrix simplifies design of electrically scanned antennas," *Electron Design*, Vol. 9, 170–173, Apr. 1961.
5. White, W., "Pattern limitations in multiple-beam antennas," *IRE transactions on Antennas and Propagation*, Vol. 10, 430–436, Jul. 1962.
6. Tseng, C.-H., C.-J. Chen, and T.-H. Chu, "A low-cost 60-GHz switched-beam patch antenna array with Butler matrix network," *IEEE Antennas and Propagation Letters*, Vol. 7, 432–435, Jul. 2008.

7. Khan, O. U., "Design of X-band 4×4 Butler matrix for microstrip patch antenna array," *TENCON'06*, 1–4, Hong Kong, Nov. 14–17, 2006.

8. Ibrahim, S. Z. and M. K. A. Rahim, "Switched beam antenna using omnidirectional antenna array," *APACE'07*, 1–4, Melaka, Malaysia, Dec. 4–6, 2007.

9. Neron, J.-S. and G.-Y. Delisle, "Microstrip EHF Butler matrix design and realization," *ETRI Journal*, Vol. 27, No. 07, 788–797, Dec. 2005.

10. El-Tager, A. M. and M. A. Eleiwa, "Design and implementation of a smart antenna using Butler matrix for ISM-band," *PIERS Proceedings*, 571–575, Beijing, China, Mar. 23–27, 2009.

11. Remez, J. and R. Carmon, "Compact designs of waveguide Butler matrices," *IEEE Antennas and Wireless Propagation Letters*, Vol. 05, 27–31, Dec. 2006.

12. Djerafi, T., N. J. G. Fonseca, and K. Wu, "Design and implementation of a planar 4×4 Butler matrix in SIW technology for wide band high power applications," *Progress In Electromagnetics Research B*, Vol. 35, 29–51, Oct. 2011.

13. Chen, C.-J. and T.-H. Chu, "Design of a 60-GHz substrate integrated waveguide Butler matrix-a systematic approach," *IEEE Transactions on Microwave Theory and Techniques*, Vol. 58, No. 07, 1724–1733, Jul. 2010.

14. Mohamed Ali, A. A., N. J. G. Fonseca, F. Coccetti, and H. Aubert, "Design and implementation of two-layer compact wideband Butler matrices in SIW technology for Ku-band applications," *IEEE Transactions on Antennas and Propagation*, Vol. 59, No. 02, 503–512, Feb. 2011.

15. Cheng, Y. J., C. A. Zhang, and Y. Fan, "Miniaturized multilayer folded substrate integrated waveguide Butler matrix," *Progress In Electromagnetics Research C*, Vol. 21, 45–58, Apr. 2011.

16. Ahmad, S. R. and F. C. Seman, "4-port Butler matrix for switched multibeam antenna array," *APACE'05*, Johor, Malaysia, Dec. 20–21, 2005.

17. Dominguez, G. E., J.-M. Fernandez-Gonzalez, P. Padilla, and M. Sierra-Castañer, "Mutual coupling reduction using EBG in steering antennas," *IEEE Antennas and Wireless Propagation Letters*, Vol. 11, 1265–1268, Dec. 2006.

18. Xu, F. and K. Wu, "Guided-wave and leakage characteristics of substrate integrated waveguide," *IEEE Transactions on Microwave Theory and Techniques*, Vol. 53, No. 01, 66–73, Jan. 2005.

19. Grigoropoulos, N., B. Sanz-Izquierdo, and P. R. Young, "Substarte integrated folded waveguides (SIFW) and filters," *IEEE Microwave and Wireless Components Letters*, Vol. 15, No. 12, 829–831, Dec. 2005.

20. Grigoropoulos, N. and P. R. Young, "Compact folded waveguides," *34th European Microwave Conference*, 973–976, Amsterdam, Oct. 12–14, 2004.

21. Pozar, D, M., *Microwave Engineering*, 4th Edition, Wiley, New York, Dec. 2011.

22. Zhai, G. H., W. Hong, K. Wu, J. X. Chen, P. Chen, J. Wei, and H. J. Tang, "Folded half mode substrate integrated waveguide 3 dB coupler," *IEEE Microwave and Wireless Components Letters*, Vol. 18, No. 08, 512–514, Aug. 2008.

23. Zhai, G. H., W. Hong, K. Wu, J. X. Chen, P. Chen, J. Wei, and H. J. Tang, "Substrate integrated folded waveguide (SIFW) narrow-wall directional coupler," *ICMMT'08*, Vol. 01, 174–177, Nanjing, China, Apr. 21–24, 2008.

24. Liu, B., W. Hong, Y. Zhang, J. X. Chen, and K. Wu, "Half-mode substrate integrated waveguide double-slot coupler," *Electronics Letters*, Vol. 43, No. 02, Jan. 2007.

25. Liu, B., W. Hong, Y. Q. Wang, Q. H. Lai, and K. Wu, "Half mode substrate integrated waveguide (HMSIW) 3-dB coupler," *IEEE Microwave and Wireless Components Letters*, Vol. 17, No. 01, 22–24, Jan. 2007.

26. Che, W., B. Fu, P. Yao, Y. L. Chow, and E. K. N. Yung, "A compact substrate integrated waveguide H-plane horn antenna with dielectric arc lens," *International Journal of RF and Microwave Computer-aided Engineering*, 473–479, Jun. 2007.

27. Wang, H., D. G. Fang, B. Zhang, and W. Q. Che, "Dielectric loaded substrate integrated waveguide H-plane horn antennas," *IEEE Transactions on Antennas and Propagation*, Vol. 58, No. 03, 640–647, Mar. 2010.